JOURNAL OF BIOMOLECULAR STRUCTURE AND DYNAMICS
2023, VOL. 41, NO. 11, 4863–4872
https://doi.org/10.1080/07391102.2022.2074139

Computational analysis of marine algal compounds for obesity management against pancreatic lipase

Lavanya Prabhakar[a], Davis G. Dicky John[a], Satya Ranjan Singh[b] and Ayaluru Murali[b]

[a]Department of Bioinformatics, Sri Ramachandra Institute of Higher Education and Research (DU), Chennai, Tamil Nadu, India; [b]Department of Bioinformatics, Pondicherry University, Puducherry, India

Communicated by Ramaswamy H. Sarma

ABSTRACT

Obesity is considered a global crisis because of its increased risk factors triggered by lifestyle changes. The prevalence of this condition is increasing at an alarming rate, giving rise to development of novel drugs. Pancreatic lipase possesses higher efficacy in inhibiting this condition among the other drug targets. In this study, virtual screening of 126 plant-derived anti-obesity compounds and 1110 marine algal compounds from seaweed metabolite database were screened and targeted against pancreatic lipase and ranked based on their binding affinity values. A total of 530 compounds that possessed best docked scores of less than −6 kcal/mol were checked for Lipinski's properties through Swiss ADME. Furthermore, these compounds were subjected to toxicity prediction using PROTOX II server. As much as 38 compounds were found to be non-toxic and were subjected to molecular docking analysis. Based on the binding energy, the following compounds RG012 (−10.15 kcal/mol), LIG42 (−9.7 kcal/mol), BC010 (−8.47 kcal/mol), RL073 (−8.2 kcal/mol), and LIG46 (−8.03 kcal/mol) were selected exhibiting higher binding affinity when compared to the standard drug (Orlistat) and hence these compounds were subjected to molecular dynamics simulation using GROMACS. BC010 complex revealed a stable interaction within the binding pocket and the binding free energy is −158.208 kJ/mol which is higher when compared to other complexes in 100 ns simulation. BC010 ((7S,11S,12S,14R)-4′,14-dimethoxyamentol) from brown algae *Cystophora fibrosa* could be considered as a potential drug candidate to suppress obesity by inhibiting pancreatic lipase.

Abbreviations: BC010: (7S,11S,12S,14R)-4′-14-dimethoxyamentol; BMI: Body Mass Index; LD50: Lethal Dose; MD: Molecular Dynamics; MM-PBSA: Molecular Mechanics/Poisson-Boltzmann Surface Area; NPT: Number of Particles, Pressure and Temperature; NVT: Number of Particles, Volume and Temperature; PL: Pancreatic Lipase; R_g: Radius of Gyration; RMSD: Root Mean Square Deviation; RMSF: Root Mean Square Fluctuation; SASA: Solvent Accessible Surface Area; SWMD: Seaweed Metabolite Database; TGs: Triglycerides

ARTICLE HISTORY
Received 3 November 2021
Accepted 30 April 2022

KEYWORDS
Obesity; pancreatic lipase; marine algal compounds; molecular docking and molecular dynamics

Introduction

With technology dependence and associated lifestyle changes, the necessity to expend calories has become imperative, especially with increased consumption of high calorie rich diets. Owing to this underlying condition, inevitable changes have been observed in people characterized by the deposition of fat which can be theoretically explained by a body mass index value (BMI) of 30 or higher (Noor et al., 2019). Obesity is mainly instigated by conditions such as imbalance between calories gained and calories expended and also environmental changes and genetic factors (Alkan et al., 2019). These changes promote chronic illness such as hyperlipidaemia, hypertension, type-2 Diabetes, and cardiovascular diseases. (Fu et al., 2016).

The inhibition of digestive enzyme activity is a significant factor in reducing body weight and pancreatic lipase (PL) is an essential enzyme that aids in the absorption of triglycerides (TGs) serving as an effective target (Ahmed et al., 2018). Lipase inhibitors decrease fat absorption by binding to the lipase enzyme in the intestine and parallelly prevents the hydrolysis of TGs to monoglycerides and fatty acids (Yun, 2010). This enzyme possesses a single chain glycoprotein consisting of 449 amino acids which is further divided into N-terminal and C-terminal domains. N-terminal being the largest serves as the catalytic domain and thereby inhibits the conversion of TGs (Bustanji et al., 2011).

The efficacy of drugs in targeting obesity was critically studied wherein Orlistat is found to regulate intestinal absorption of fat by inhibiting PL (Heck et al., 2000). It is derived from lipstatin, a natural product of *Streptomyces toxytricini* which binds covalently at the catalytic triad of PL directed to the serine residue and aids in inhibition of PL (Carrie, 2001). Intake of Orlistat leads to several side effects

CONTACT Davis G. Dicky John dicky@sriramachandra.edu.in Department of Bioinformatics, Sri Ramachandra Institute of Higher Education and Research (DU), Chennai, Tamil Nadu, India

Supplemental data for this article can be accessed online at http://dx.doi.org/10.1080/07391102.2022.2074139.

such as constipation, hypertension, insomnia, headache and dryness in mouth (Yun, 2010) yet it is still being prescribed and is considered acceptable. As a result of these ill effects, there is an urge to explore the available natural resources to curb obesity.

Seaweeds, belonging to the marine ecosystem, provides necessary nutritional and dietary factors which may create a revolutionary impact in the development of an effective and safe alternate therapy for obesity. Marine organisms are found to possess novel metabolites which are widely explored in drug research development; of this 25% is extensively contributed from algal source (Davis & Vasanthi, 2015). The marine diversity has rich source of fucoxanthin, potassium, dietary fibre and non-starch polysaccharides (Carrageenan and Alginic acid) (Murai et al., 2021) thereby providing functional benefits when compared to the other available resources (Hu et al., 2016). Active components from seaweeds may act against obesity by i) interfering with digestive enzyme activity ii) enhancing expenditure of energy and thereby decreasing adipogenesis iii) suppressing appetite iv) increasing fat excretion by altering the composition of intestinal microbiota (Fu et al., 2016).

The current research is on data mining of compounds having activity against PL from plant sources and compounds in the Seaweed Metabolite Databases (SWMD). Based on drug likeness and toxicity analysed, *in silico* molecular docking analysis for the compounds was performed. In addition to this, the identified potential compounds were subjected to molecular dynamics (MD) simulation study to understand the conformational changes and also to determine the binding stability with PL. Finally, the MM-PBSA (molecular mechanics/Poisson-Boltzmann surface area) calculation estimated binding free energies of protein ligand docked complexes.

Methodology

Protein preparation

The three-dimensional structure of PL with a resolution of 2.46 Å (PDB ID: 1LPB) was retrieved from the Protein Data Bank (Egloff et al., 1995). This 3D structure comprises two chains: Chain A and chain B - of which chain B possesses 449 amino acid sequences from humans that was utilized as a potential source of target in docking-simulation studies. Protein preparation was carried out using UCSF Chimera; water molecules, ligands, non-interacting ions and chain A were removed from 1LPB protein structure prior to virtual screening.

Preparation of ligand

The compounds mentioned in this work were retrieved from two different sources: (i) extensive literature mining was used to retrieve 126 compounds derived from plant-based sources targeting against PL (Table S1, supplementary material) and (ii) marine algae containing 1110 ligands were downloaded from Seaweed Metabolite Database in mol format (Davis & Vasanthi, 2011). The 3D structures of these ligand molecules were generated using Corina demo (https://www.mn-am.com/online_demos/corina_demo_interactive)

Virtual screening

The structure based virtual screening was executed using Autodock vina v1.1.2 (Trott & Olson, 2010) with PyRx v0.8 software (Dallakyan & Olson, 2015). Generally, during the process of docking, ligands were contemplated to be flexible and the target molecule being rigid. The ligands were energy minimized in PyRx software using the UFF force field. The optimization was carried out using a conjugate gradient algorithm. The docking site was defined by the methoxyundecylphosphinic (MUP) acid from the same 1LPB structure data (Egloff et al., 1995). Exhaustiveness was set on 8, wherein unique poses were generated for each ligand. The binding energy corresponding to RMSD/ub and RMSD/lb of zero (least), was selected as it possessed a good binding pose for further validation using Autodock 4.0. (Morris et al., 1998).

Analysis of drug likeness

Drug likeness is a pharmacokinetic property examined to analyse the function of the compound within the human framework by employing Swiss ADME (Daina et al., 2017). Molecular mass, lipophilicity, sum of hydrogen bond donors/acceptors and number of rotatable bonds were evaluated based on Lipinski's rule of five (RO5) and those compounds that does not fit well to this may not possess drug-like properties and also tend to have lesser bioavailability. (Lipinski et al., 2001).

Toxicity prediction

The toxicity of selected compounds was evaluated to identify the drugs that are least toxic for human consumption. Protox II, a virtual lab server, was used to predict median lethal dose (LD50) values in mg/kg body weight (Banerjee et al., 2018). Globally Harmonized System of classification of labelling of chemicals (GHS, United Nations, first revised edition 2005) was employed wherein the toxicity class ranges from I to VI and the input compound were classified based on the toxicity level. The class 6 compounds which possess LD50 values greater than 5000 were found to be non-toxic and indicated the effectiveness based on their prediction score (Drwal, 2014).

Molecular docking

Molecular docking approach for the chosen 38 natural compounds along with a standard drug (Orlistat) against 1LPB was validated using Autodock 4.2.6 with ADT tools of 1.5.6 version (Morris et al., 1998). Initially, water molecules and hetero atoms were removed followed by addition of polar hydrogen atoms. Kollaman charges were computed for the receptor. Gasteiger charges were assigned to energy minimized conformations of ligands. The torsion tree and the

number of rotatable bonds were defined for the ligand. The protein and ligand in the workspace were then saved in PDBQT format. Lamarckian genetic algorithm parameters were set to '2500000' for maximum number of energy evaluation, '27000' for maximum number of generations, '1' for maximum number of top individuals, '0.02' as mutation rate, '0.8' as crossover rate, population size of 300 and 100 Long GA runs. The results were analysed based on their binding energies and interactions with amino acids PHE77, SER152, and HIS263 for further validation. The output was built using UCSF Chimera v1.15 software to render receptor ligand complexes (Pettersen et al., 2004). The docked complexes were visualized using BIOVIA Discovery studio client 2020 (DassaultSystèmes BIOVIA, Discovery Studio Modelling Environment, Release 2017, San Diego: Dassault Systèmes, 2016).

Molecular dynamics (MD) simulation study

The native/apo-enzyme of PL and its complexes with five individual PL-ligands and one reference ligand docking complex were selected for MD simulation using the software GROMACS 5.1.4 (James, 2015) (Groningen Machine for Chemical Simulations) in GROMOS96 54a7 force field (Schmid et al., 2011) for 100 ns. PRODRG server (Schüttelkopf & van Aalten, 2004) was used to generate the parameters and topologies files for each ligand. Native protein, along with its complex with the selected five most effective ligands and reference ligand, were simulated with a $11.128 \times 11.128 \times 11.128$ (nm)—cubic box and SPCE water-filled model (Wu et al., 2006). A total of 43,714, 42,783, 42,787, 42,778, 42,784, 42,789, and 42,781 solvent molecules were added to each system, i.e. BC010, LIG46, RG012, LIG42, RL073, Orlistat and native protein, respectively. Neutralization of the system was carried out by adding 3 Na^+ ions, and the energy minimization was done by using the 50,000 steepest descent method using a Fourier grid. The particle mesh Ewald (PME) method was used with a 1.2 nm cut-off and a Fourier spacing of 0.16 nm for short-range electrostatic interactions. After energy minimization of each complex of PL, the NVT (at a constant number of particles, volume, and temperature) with modified Berendsen thermostat with rescaling of velocity (Bussi et al., 2007) 310 K and with a time step of 0.1 ps, PME coulomb type for short-range electrostatic interactions with Fourier spacing of 0.16 nm for 100 ps time scale. The NPT (at a constant number of particles, pressure, and temperature) Parrinello–Rahman pressure coupling (Martonák et al., 2003) at 1 bar with a 4.5×10^{-5} bar^{-1} compressibility equilibrations and with a time constant of 2 ps were performed for equilibrating the system for 100 ps time scale. The final MD step for each of the equilibrated PL systems was performed for a 100 ns time scale with time steps of 2 fs and bond lengths were constrained by Linear Constraint Solver (LINCS) algorithm (Hess et al., 2008).

MM/PBSA binding free energy calculation

The binding free energy calculation is another advanced computational analysis to understand the contribution of the binding energy of each amino acid and dynamic behaviours in the individual protein-ligand complex. The MM/PBSA-based binding free energy (ΔG_{bind}) of each simulated docking complex was calculated with the g_mmpbsav5.12 package in the GROMACS platform (Kumari et al., 2014).

Results and discussion

Virtual screening

The virtual screening of 1236 compounds against 1LPB target protein was done using PyRx v0.8 software. The docked molecules with binding energy value less than –6 kcal mol^{-1} were selected for further assessment. Out of 1236 compounds, 530 compounds showing binding energy less than –6 kcal mol^{-1} is shown in Table S2 (supplementary material). The docking protocol was validated by docking the co-crystalized ligand MUP into the active site of 1LPB. The superimposed pose of docked and co-crystallized ligand are given in Figure S1 (supplementary material).

Drug likeness

Further 530 compounds that had good binding affinity were subjected to ADME screening and it was observed that 443 compounds were Lipinski's complaint. The drug likeness properties for 443 compounds are represented in Table S3 (supplementary material).

Toxicity prediction

The Canonical SMILES format of 443 compounds were incorporated as input file and tested using PROTOX II server for toxicity prediction. It was observed that only 38 compounds were non-toxic based on the labelling of chemical classes (Drwal, 2014). The toxicity level along with LD50 values in mg/kg are listed in Table S4 (supplementary material).

Docking studies

Molecular docking study was carried out for 38 compounds against PL (1LPB) and the interactions were given in Table S5 (supplementary material). Orlistat being a standard drug serves as a suitable reference against PL which inhibits hydrolysis of TGs. (Heck et al., 2000). Five lead compounds showed best docked pose, of which two compounds (LIG46 and LIG42) were based out of plant origin and three compounds (RG012, RL073 and BC010) were derived from algal source. These compounds were found to possess higher binding affinity when compared to the reference molecule (Orlistat). The binding energies of the above-mentioned compounds and also their energy interaction with the key residues are summarized in Table 1.

The docking results obtained pointed out that Orlistat had three conventional hydrogen bonds with PHE77, SER152 and HIS263 and a single carbon hydrogen bond with ALA259 (Figure 1(a)).

Table 1. Binding energy and interactions of ligands docked with pancreatic lipase.

				Interactions with amino acid residues of 1LPB		
Compound name	Compound name	Compound structure	Binding energy (kcal/mol)	Hydrogen bond interactions	Hydrophobic interaction	Pi interactions
Orlistat	Stranded drug against pancreatic lipase	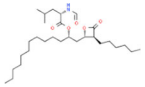	–4.89	PHE77, SER152, HIS263, ALA259	PHE77, ILE78, TYR114, PRO180, ILE209, VAL210, LEU213, PHE215, TRP252, ARG256, LEU264	–
RG012	6β,24ε-Dihydroxycholesta-4, 25-dien-3-one	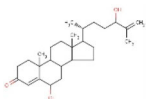	–10.15	PHE77, HIS151, ARG256	–	PHE215
LIG42	Diosgenin	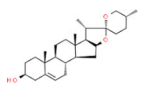	–9.7	–	PHE77, ILE78, TYR114, PHE215, ARG256, ALA259, ALA260 and LEU264	–
BC010	(7S,11S,12S,14R)-4′, 14-Dimethoxyamentol)	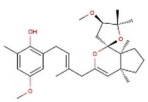	–8.47	HIS263, PHE77	TYR114, HIS151, ALA259, ALA260, LEU264	–
RL073	2-Hydroxyluzofuranone	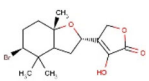	–8.2	PHE77, SER152, HIS263	ALA178, PRO180, ILE 209	TYR114, PHE215
LIG46	Epicatechin	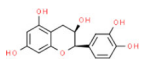	–8.03	GLY76, ASP79, HIS151, SER152, PRO180, PHE215, HIS263,	ALA178	TYR114, PHE215, HIS263

Table 2. Energy contribution of protein-ligand complexes calculated using MM/PBSA method.

Energy parameter (kJ/mol)	RG012	BC010	RL073	LIG42	LIG46	Orlistat
Binding energy	−85.1 ± 11.9	−158.2 ± 11.4	−101.7 ± 11.7	−71.6 ± 2.5	−108.8 ± 17.6	−23.0 ± 2.5
Electrostatic energy	−22.1 ± 10.6	−10.2 ± 4.0	−29.5 ± 6.6	−8.4 ± 0.3	−6.3 ± 4.1	−6.8 ± 0.5
Polar solvation energy	57.9 ± 19.2	74.0 ± 12.6	72.3 ± 10.8	37.3 ± 1.2	86.8 ± 14.9	22.7 ± 1.4
SASA energy	−13.0 ± 1.8	−20.0 ± 1.4	−13.8 ± 0.8	−10.0 ± 0.2	−16.5 ± 0.7	−3.8 ± 0.3
Van der Waal energy	−107.8 ± 14.5	−202.0 ± 14.2	−113.6 ± 10.7	−90.3 ± 2.4	−172.8 ± 9.1	−35.0 ± 2.6

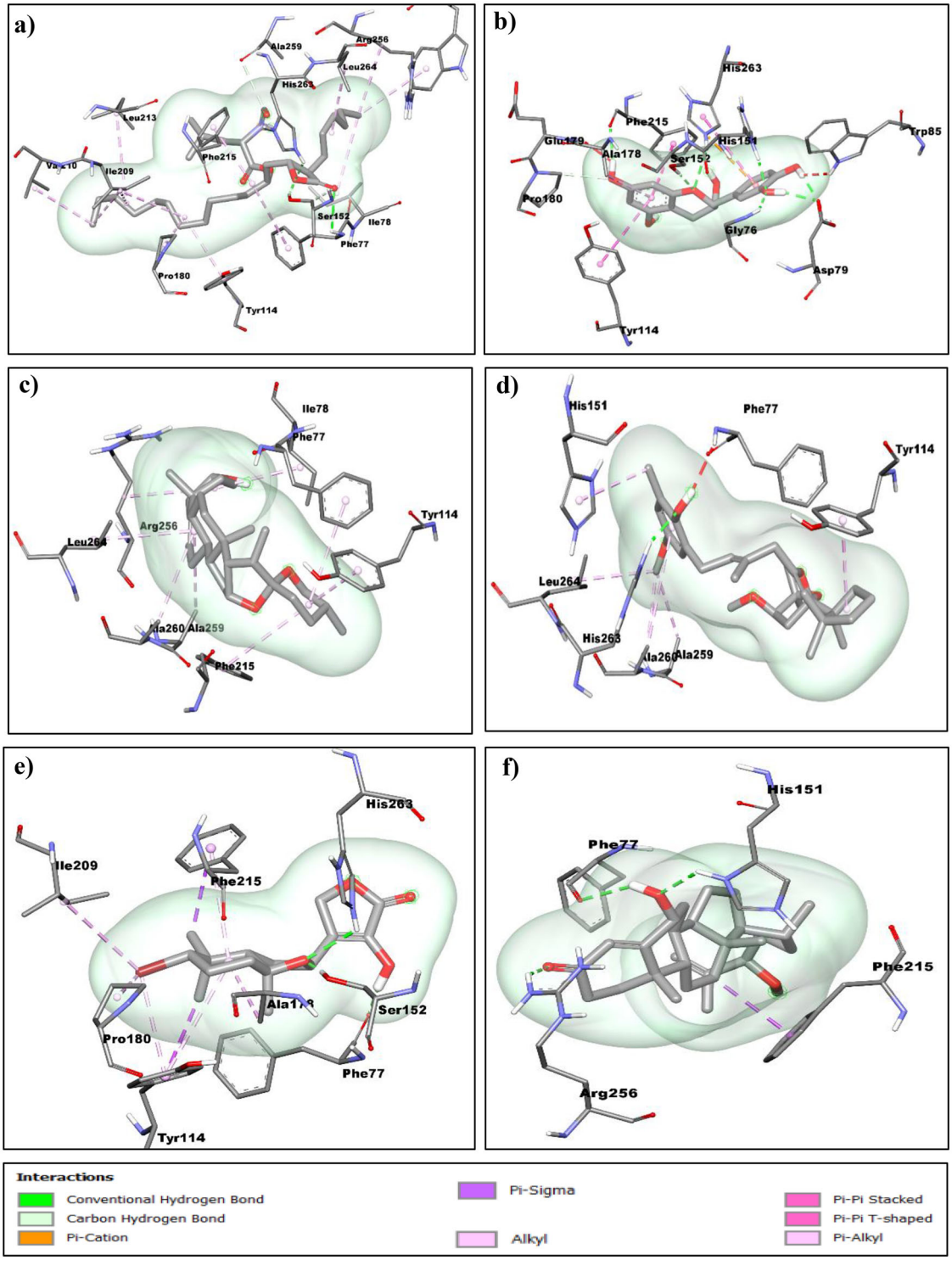

Figure 1. 3D interactions of ligand and pancreatic lipase complexes. a) Orlistat, b) LIG46, c) LIG42, d) BC010, e) RL073 and f) RG012.

LIG46 (Epicatechin), a flavonoid from *Salacia reticulata*, has an inhibitory activity against PL (Nakai et al., 2005) by slowing down the absorption of triacylglycerol which induces suppression of postprandial hypertriacylglycerolemia (Ikeda et al., 2005; Sahib et al., 2011). The docking results obtained pointed out that LIG46 had a single carbon hydrogen bond

with PRO180 and six conventional hydrogen bonds with GLY76, ASP79, HIS151, SER152, PHE215 and HIS263 residues (Figure 1(b)). LIG42 (Diosgenin) from *Dioscorea nipponica makino* belongs to the class of terpenes reported potent inhibitory activity against PL (Kwon et al., 2003). The conformational binding of LIG42 exhibited binding energy of –9.7 kcal/mol which possessed hydrophobic interactions with PHE77, ILE78, TYR114, PHE215, ARG256, ALA259, ALA260 and LEU264 (Figure 1(c)).

BC010 ((7S,11S,12S,14R)-4′-14-dimethoxyamentol), a brown alga from *Cystophora fibrosa* belonging to the tetraprenyltoluquinols class of compounds (Laird & Van Altena, 2006) exhibited binding energy of –8.47 kcal/mol and one conventional hydrogen bond with HIS263 residue. It also exhibited hydrophobic interactions with TYR 114, HIS 151, ALA 259, ALA 260, LEU 264 residues (Figure 1(d)).

Red algae were found to possess anti-lipase activity as reported by (Bitou et al., 1999) and (Kannan, 2014). RL073 (2-hydroxyluzofuranone), a sesquiterpene from *Laurencia saitoi* (red algae), (Su et al., 2009) possessed binding energy of –8.2 kcal/mol (Figure 1(e)). RG012 (6β,24ε-Dihydroxycholesta-4,25-dien-3-one) from *Galaxaura marginata* (red alga) classified under oxygenated desmosterols (Sheu et al., 1997) showed highest binding energy of –10.15 kcal/mol (Figure 1(f)).

Overall docking results revealed that five selected compounds along with Orlistat had hydrogen and hydrophobic interactions with common residues such as PHE77, TYR114, HIS151, SER152, PRO180, PHE215, ARG256, HIS263 and

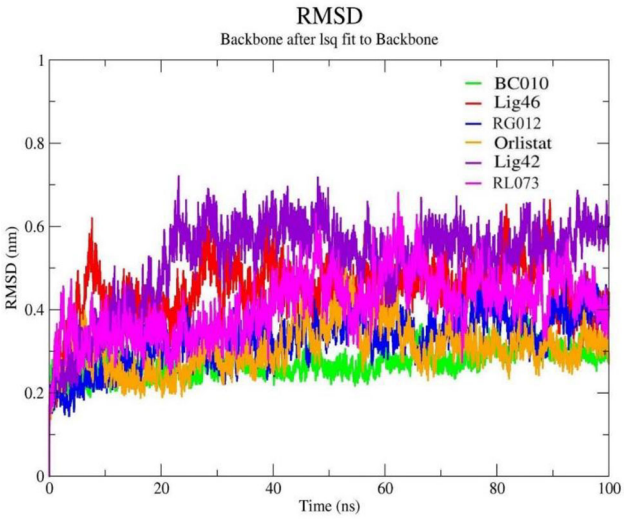

Figure 2. RMSD of PL backbone associated with all PL-complexes.

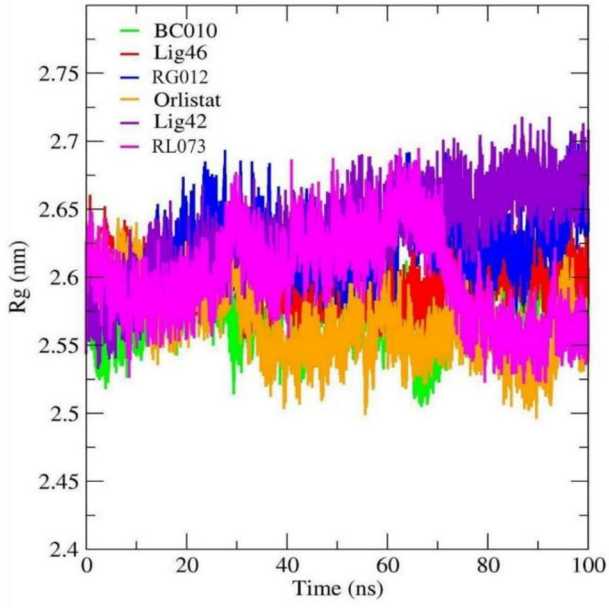

Figure 4. Radius of gyration of PL in complexes.

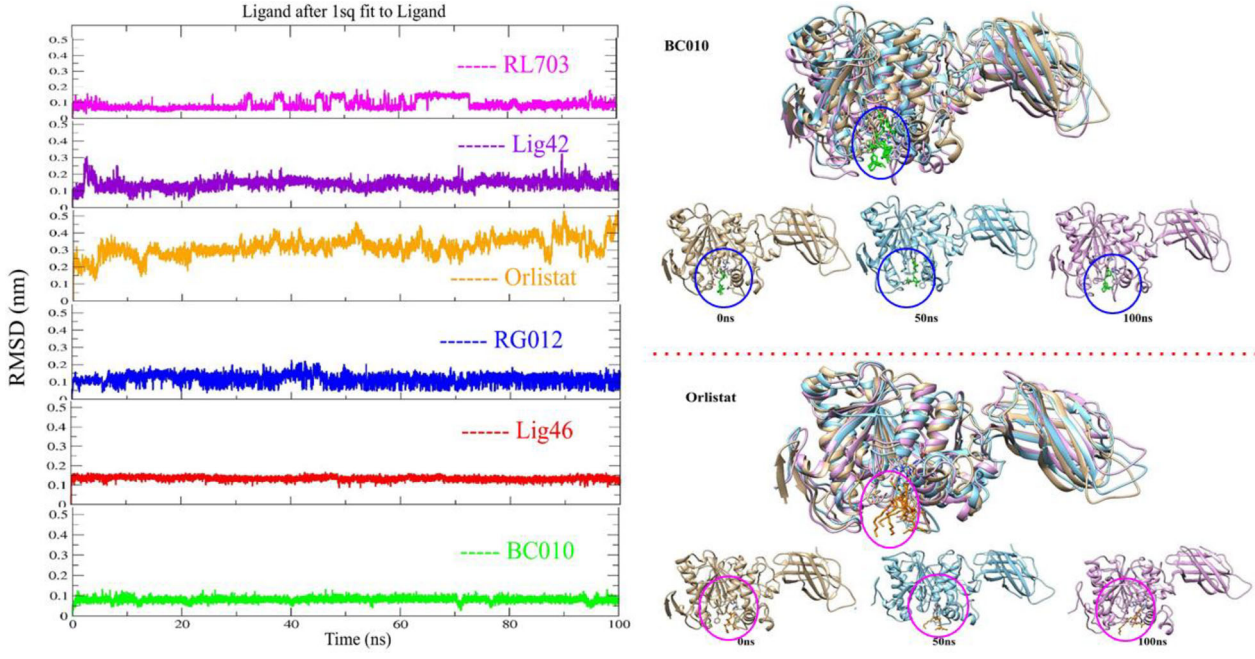

Figure 3. a) RMSD of ligand molecules associated with all PL-complexes, overlay and tile conformation of b) PL-BC010—blue colored circle are presenting the position of BC010, c) PL-orlistat complexes—pink colored circle are presenting the orlistat position at 0, 50 and 100 ns.

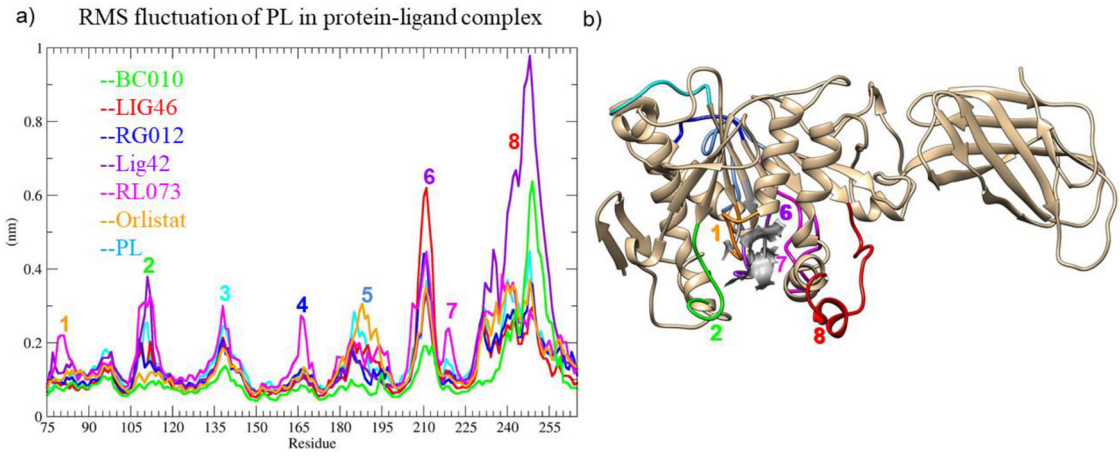

Figure 5. a) RMSF of PL associated with all PL-complexes and apoenzyme, b) highest peak near the binding site (no. 1, 2, 6, 7, 8) shown in different color.

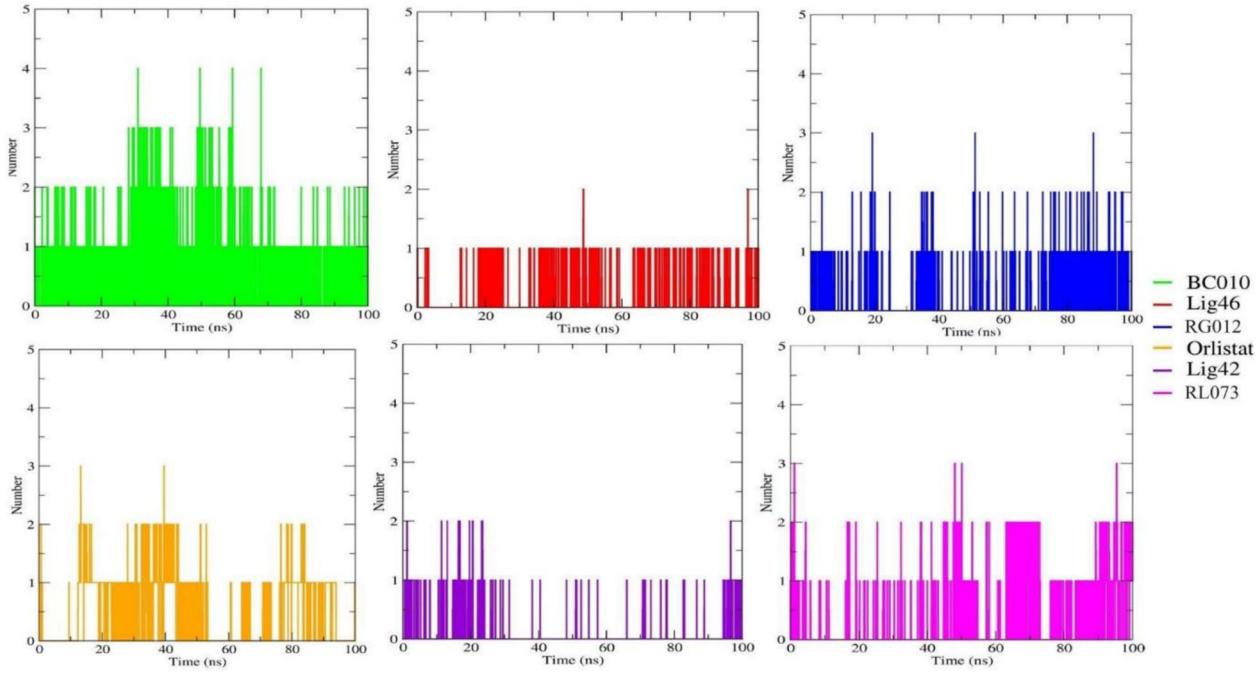

Figure 6. Hydrogen bond distribution of PL-complexes.

LEU264. It was noted that these residues were also found in the active sites of PL. PHE 77, HIS 152, SER263 were the most common residues which is similar to orlistat interaction with PL. Although LIG42 and LIG46 were found to be potent against PL, RG012 compound from marine seaweed exhibited best affinity with target protein and also possessed lower binding energy in comparison with plant derived and a reference molecule.

Molecular dynamics (MD) simulation of docked protein-ligand complexes

Molecular dynamics simulation was employed to assess stability and its interaction- dynamics of protein-ligand complexes. The structural stability of the native protein PL with the selected five protein-ligand docking complexes (RG012, LIG46, LIG42, BC010 and RL073) were analysed through the RMSD-protein backbone, RMSF-C-alpha and Rg-score of protein by MD simulation.

The RMSD of the protein backbone in all selected five complexes at 100 ns is represented in Figure 2. The ligand RMSD plot elucidates stable dynamic profiles were observed in an average of 0.9 Å for marine compounds (BC010, RG102, RL073) and 1.35 Å for plant-based molecules (LIG46 and LIG42). The RMSD plot for ligand Orlistat showed a greater average deviation of 3.1 Å due to the presence of an aliphatic side chain, while both marine and plant-based compounds were stable.

For further verifying the ligand stability at the binding region of PL, PL-BC010 (best among all ligands) and PL-orlistat (FDA approved drug) complexes were extracted at 0, 50 and 100 ns time frames (Figure 3(a,b)). It has been shown that the change in position of the BC010 ligand in PL-BC010 is more stable at binding site of PL at these three-time frames rather than of orlistat molecule in PL-orlistat complex.

The radius of gyration, Rg, plots exhibit the level of compactness of PL-associated complexes and are depicted in Figure 4. BC010 possessed a lesser gyration value among all

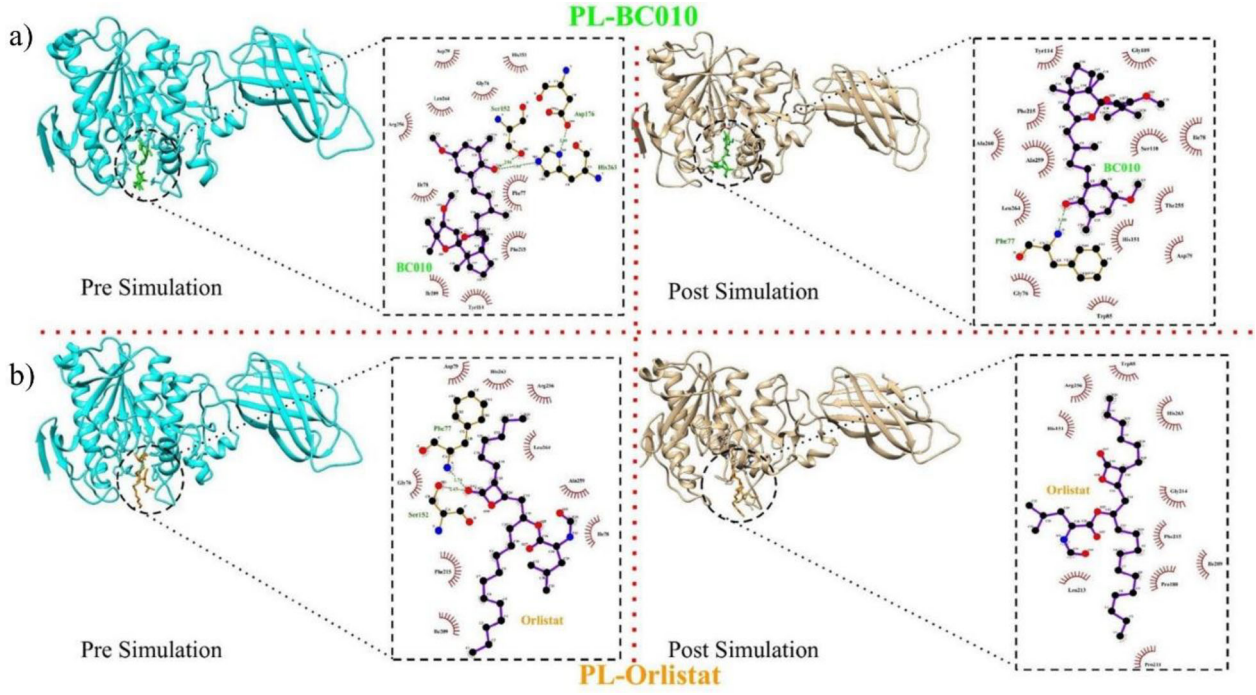

Figure 7. Pre and postsimulation interaction analysis of a) PL-BC010 and b) PL-orlistat.

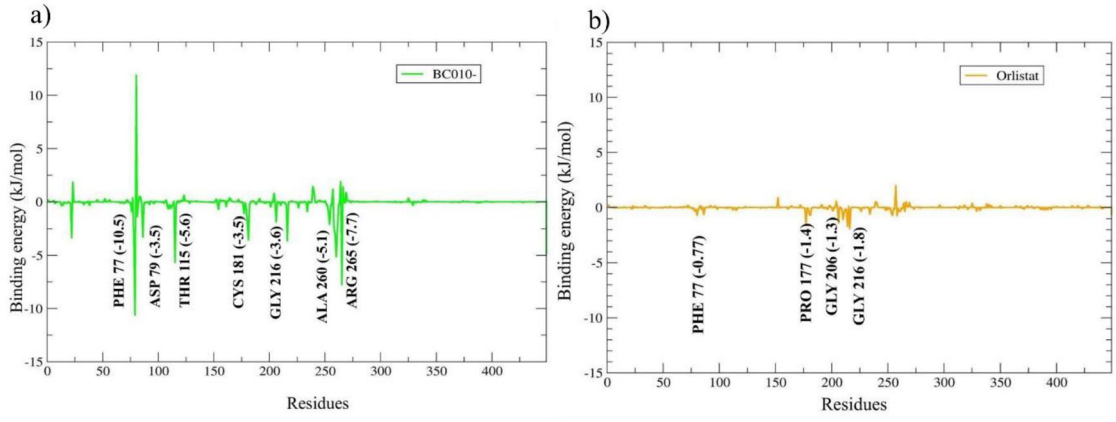

Figure 8. Energy contribution per residue of a) PL-BC010 complex b) PL-orlistat.

complexes which showed that BC010 had closed conformation. Conversely, LIG42 had open conformation. The results depicted that BC010 had smaller Rg-value than other complexes as shown in Figure 4. This lower Rg has shown in BC010 associated PL, which can form a narrow cavity (more constraints) at the binding region thereby it reduced the ligand dynamism seen in BC010. The higher Rg has shown in LiG42 associated PL, which can form a broader cavity (less constraint) at the binding region and hence showed the relatively high dynamism in LIG42.

Root mean square fluctuation (RMSF) is calculated for Cα atoms of protein residues to analyze the backbone structure flexibility. The residues that fluctuate during the simulation time for 100 ns are depicted by the peaks in the RMSF plot (Figure 5(a)). RMSF analyzes showed that marine algal compounds showed less residual fluctuation when compared to plant-derived and reference complexes. Whereas BC010 complex exhibited less residual fluctuation throughout the simulation. Figure 5(b) includes the secondary structure elements that were showing higher fluctuations and were surrounded by the binding regions.

The specific interaction between protein-ligand docked complexes was analysed using H-bond interaction and is represented in Figure 6. H-bond analysis portrays that marine algal compound have more H-bonds than plant-derived compounds and Orlistat with PL. Apart from that, the BC010 molecule exhibited a stable H-bond pattern compared to all other natural compounds including Orlistat throughout the MD-simulation periods. Also, to verify the post-simulation interaction study of both PL-BC010—best among all ligands (Figure 7(a)) and PL-orlistat—control (Figure 7(b)) complex, the final time frame (100 ns) structure of both complexes was dumped and analysed the H-bond interactions pattern. The post-simulation interaction analysis in PL-BC010 reveals that the H-bond between PHE 77 and BC010 is intact with a 3 Å H-bond length and present at the binding site of PL.

Whereas in PL-orlistat complex, Orlistat is not intact with a single H-bond with PL.

MM/PBSA and binding free energy per residue analysis

The MM/PBSA calculation for all protein-ligand complexes to compute the binding energy during the MD simulation was executed. Binding affinity with other energies such as Van der Waal energy, electrostatic energy, polar solvation energy, and solvent accessible surface area (SASA) energy were calculated for each docking complex between 90 to 100 ns at a 0.1 ns time step (Table 2). Comparatively, Orlistat-PL presented the minimum binding energy, −23.028 kJ/mol, whereas the remaining compounds such as BC010-PL, RG012-PL, RL073-PL, LIG42-PL, and LIG46-PL computed binding energies correspondingly −158.208, −85.179, −101.878, −71.608, −108.873 kJ/mol (Table 2). The binding free energy calculation of each complex in between 90 and 100 ns was represented in a graphical presentation (Figures S1–S6, supplementary material) which implies the importance of the binding of ligands towards the complex formation.

The total binding energy contribution in residue-wise for protein-ligand complexes were subtracted using MM/PBSA calculation and is depicted in Figures S7–S10 (supplementary material). Overall, BC010 and Orlistat potential against obesity presented the energy per residues calculation in a graph format (Figure 8(a,b)), from which BC010 marine formed more interaction than other ligand molecules within 100 ns. There are two common residues (PHE 77 and GLY 216) in PL-BC010 and PL-orlistat. But the residues PHE77 (–10.5) and GLY216 (–3.6) show greater binding affinity in PL-BC010 complex formation in comparison with PL-orlistat {PHE77 (–0.77) and GLY216 (–1.8)}. Thus, marine products, especially BC010, exhibited stronger binding energy with PL (PHE77) than plant-based compounds and Orlistat within 100 ns confirms from both pre- and post-simulation analysis.

Conclusion

Virtual screening of 126 plant derived anti-obesity compounds and 1110 marine algal compounds from SWMD was done against PL. Docking studies revealed that three marine-based compounds (BC010, RG012, RL073) and two plant-derived compounds (LIG42 and LIG46) possessed the best docked pose with least binding affinity towards active site residues of PL. Furthermore, it was concluded that BC010-PL complex has shown significant binding energy in comparison to plant-based compounds and Orlistat throughout the simulation time of 100 ns. Owing to the bioavailability, drug likeness and toxicity prediction of this compound can be explored further as a potential drug target to treat obesity. In addition, it was noted that BC010 (7S,11S,12S,14R)-4′-14-dimethoxyamentol), the lead component belongs to the group of tetraprenyltoluquinols isolated from brown algae found to possess antioxidant activity. It was also reported that marine algal compounds are responsible for the inhibition of lipid oxidation (Seo et al., 2006). Thus, computational approach illustrates that BC010 (7S,11S,12S,14R)-4′-14-dimethoxyamentol) is a potent inhibitor against PL.

Disclosure statement

The authors declare no conflict of interest.

Funding

This research work was funded by Sri Ramachandra Institute of Higher Education and Research under grant of Founder-Chancellor Shri. N.P.V. Ramasamy Udayar Research Fellowship.

ORCID

Satya Ranjan Singh http://orcid.org/0000-0003-0639-4453
Ayaluru Murali http://orcid.org/0000-0001-6406-6840

References

Ahmed, B., Ali Ashfaq, U., & Usman Mirza, M. (2018). Medicinal plant phytochemicals and their inhibitory activities against pancreatic lipase: molecular docking combined with molecular dynamics simulation approach. *Natural Product Research*, *32*(10), 1123–1129. https://doi.org/10.1080/14786419.2017.1320786

Alkan, I., Zuhal Altunkaynak, B., Altun, G., & Erener, E. (2019). On the hypothalamic levels of fat mass/obesity- associated protein and neuropeptide Y in obese the investigation of the effects of topiramate on the hypothalamic levels of fat mass/obesity-associated protein and neuropeptide y in obese female rats. *Nutritional Neuroscience*, *22*(4), 243–1415. https://doi.org/10.1080/1028415X.2017.1374033

Banerjee, P., Eckert, A. O., Schrey, A. K., & Preissner, R. (2018). ProTox-II: A webserver for the prediction of toxicity of chemicals. *Nucleic Acids Research*, *46*(W1), W257–63. https://doi.org/10.1093/nar/gky318

Bitou, N., Ninomiya, M., Tsujita, T., & Okuda, H. (1999). Screening of lipase inhibitors from marine algae. *Lipids*, *34*(5), 441–445. https://doi.org/10.1007/s11745-999-0383-7

Bussi, G., Donadio, D., & Parrinello, M. (2007). Canonical sampling through velocity rescaling. *The Journal of Chemical Physics*, *126*(1), 014101. https://doi.org/10.1063/1.2408420

Bustanji, Y., Al-Masri, I. M., Mohammad, M., Hudaib, M., Tawaha, K., Tarazi, H., & Alkhatib, H. S. (2011). Pancreatic lipase inhibition activity of trilactone terpenes of ginkgo biloba pancreatic lipase inhibition activity of trilactone terpenes of *Ginkgo biloba*. *Journal of Enzyme Inhibition and Medicinal Chemistry*, *26*(4), 453–459. https://doi.org/10.3109/14756366.2010.525509

Carrie, R. I. C. (2001). Inhibition of gastrointestinal lipolysis by orlistat during digestion of test meals in healthy volunteers. *American Journal of Physiology-Gastrointestinal and Liver Physiology*, *281*(1), 16–28. https://doi.org/10.1152/ajpgi.2001.281.1.G16

Daina, A., Michielin, O., & Zoete, V. (2017). SwissADME : A free web tool to evaluate pharmacokinetics, drug- likeness and medicinal chemistry friendliness of small molecules. *Nature Publishing Group*, January:1–13. https://doi.org/10.1038/srep42717.

Dallakyan, S., & Olson, A. J. (2015). Participation in global governance: Coordinating the voices of those most affected by food insecurity. *Global Food Security Governance*, *1263*, 1–11. https://doi.org/10.1007/978-1-4939-2269-7_19.

Davis, G. D. J., & Vasanthi, A. H. R. (2011). Seaweed Metabolite Database (SWMD): A database of natural compounds from marine algae bioinformation. *Bioinformation*, *5*(8), 361–364. https://doi.org/10.6026/97320630005361

Davis, G. D. J., & Vasanthi, A. H. R. (2015). QSAR based docking studies of marine algal anticancer compounds as inhibitors of protein kinase B

(PKBβ). *European Journal of Pharmaceutical Sciences*, *76*, 110–118. https://doi.org/10.1016/j.ejps.2015.04.026

Drwal, M. N., Banerjee, P., Dunkel, M., Wettig, M. R., & Preissner R. (2014). ProTox: A web server for the in-silico prediction of rodent oral toxicity. *Nucleic Acids Research*, *42*, 53–58. http://dx.doi.org/10.1093/nar/gku401.

Egloff, M. P., Marguet, F., Buono, G., Verger, R., Cambillau, C., & van Tilbeurgh, H. (1995). A resolution structure of the pancreatic lipase-colipase complex. *Biochemistry*, *34*(9), 2751–2762. https://doi.org/10.1021/bi00009a003

Fu, C., Jiang, Y., Guo, J., & Su, Z. (2016). Natural products with anti-obesity effects and different mechanisms of action. *Journal of Agricultural and Food Chemistry*, *64*(51), 9571–9585. https://doi.org/10.1021/acs.jafc.6b04468

Heck, A. M., Yanovski, J. A., & Calis, K. A. (2000). Orlistat, a new lipase inhibitor for the management of obesity. *Pharmacotherapy*, *20*(3), 270–279. https://doi.org/10.1592/phco.20.4.270.34882

Hess, B., Kutzner, C., van der Spoel, D., & Lindahl, E. (2008). GROMACS 4: Algorithms for highly efficient, load-balanced, and scalable molecular simulation. *Journal of Chemical Theory and Computation*, *4*(3), 435–447. https://doi.org/10.1021/ct700301q

Hu, X., Tao, N., Wang, X., Xiao, J., & Wang, M. (2016). Marine-derived bioactive compounds with anti-obesity effect: A review. *Journal of Functional Foods*, *21*, 372–387. https://doi.org/10.1016/j.jff.2015.12.006

Ikeda, I., Tsuda, K., Suzuki, Y., Kobayashi, M., Unno, T., Tomoyori, H., Goto, H., Kawata, Y., Imaizumi, K., Nozawa, A., & Kakuda, T. (2005). Biochemical and molecular actions of nutrients tea catechins with a galloyl moiety suppress postprandial hypertriacylglycerolemia by delaying lymphatic transport of dietary fat in rats. *The Journal of Nutrition*, *135*(2), 155–159. https://doi.org/10.1093/jn/135.2.155

James, M. (2015). GROMACS: High performance molecular simulations through multi-level parallelism from laptops to supercomputers. *Science Direct*, 1–7. https://doi.org/10.1016/j.softx.2015.06.001.

Kannan, M. (2014). Antibacterial and antiobesity activities of marine algae *Gracilaria corticata* and *Spirulina platensis*. *International Journal of Pharmacy and Pharmaceutical Sciences*, *6*(6), 4–8.

Kumari, R., Kumar, A., & Lynn, R., Open Source Drug Discovery Consortium. (2014). g_mmpbsa-a GROMACS tool for high-throughput MM-PBSA calculations . *Journal of Chemical Information and Modeling*, *54*(7), 1951–1962. https://doi.org/10.1021/ci500020m

Kwon, C.-S., Sohn, H. Y., Kim, S. H., Kim, J. H., Son, K. H., Lee, J. S., Lim, J. K., & Kim, J.-S. (2003). Anti-obesity effect of *Dioscorea nipponica* makino with lipase-inhibitory activity in rodents. *Bioscience, Biotechnology, and Biochemistry*, *67*(7), 1451–1456. https://doi.org/10.1271/bbb.67.1451

Laird, D. W., & Van Altena, I. A. (2006). Tetraprenyltoluquinols from the brown alga *Cystophora fibrosa*. *Phytochemistry*, *67*(10), 944–955. https://doi.org/10.1016/j.phytochem.2006.03.011

Lipinski, C. A., Lombardo, F., Dominy, B. W., & Feeney, P. J. (2001). Experimental and computational approaches to estimate solubility and permeability in drug discovery and development settings. *Advanced Drug Delivery Reviews*, *46*(1–3), 3–26. https://doi.org/10.1016/S0169-409X(00)00129-0

Martonák, R., Laio, A., & Parrinello, M. (2003). Predicting crystal structures: The Parrinello-Rahman method revisited. *Physical Review Letters*, *90*(7), 075503. https://doi.org/10.1103/PhysRevLett.90.075503

Morris, G. M., Goodsell, D. S., Halliday, R. S., Huey, R., Hart, W. E., Belew, R. K., & Olson, A. J. (1998). Automated Docking using a Lamarckian genetic algorithm and an empirical binding free energy function. *Journal of Computational Chemistry*, *19*(14), 1639–1662. https://doi.org/10.1002/(SICI)1096-987X(19981115)19:14<1639::AID-JCC10>3.0.CO;2-B

Murai, U., Yamagishi, K., Kishida, R., & Iso, H. (2021). Impact of Seaweed intake on health. *European Journal of Clinical Nutrition*, *75*(6), 877–889. https://doi.org/10.1038/s41430-020-00739-8

Nakai, M., Fukui, Y., Asami, S., Toyoda-Ono, Y., Iwashita, T., Shibata, H., Mitsunaga, T., Hashimoto, F., & Kiso, Y. (2005). Inhibitory effects of oolong tea polyphenols on pancreatic lipase in vitro. *Journal of Agricultural and Food Chemistry*, *53*(11), 4593–98. https://doi.org/10.1021/jf047814+

Noor, Z. I., Ahmed, D., Rehman, H. M., Qamar, M. T., Froeyen, M., Ahmad, S., & Mirza, M. U. (2019). Analysis of *Ocimum basilicum* aerial biomass and *in silico* molecular docking simulations with. *Biology*, *8*(4), 92–20. https://doi.org/10.3390/biology8040092

Pettersen, E. F., Goddard, T. D., Huang, C. C., Couch, G. S., Greenblatt, D. M., Meng, E. C., & Ferrin, T. E. (2004). UCSF Chimera-a visualization system for exploratory research and analysis. *Journal of Computational Chemistry*, *25*(13), 1605–1612. https://doi.org/10.1002/jcc.20084

Sahib, N. G., Hamid, A. A., Kitts, D., Purnama, M., Saari, N., & Abas, F. (2011). The effects of *Morinda citrifolia, Momordica charantia and Centella asiatica* extracts on lipoprotein lipase and 3t3-l1 preadipocytes najla. *Journal of Food Biochemistry*, *35*(4), 1186–1205. https://doi.org/10.1111/j.1745-4514.2010.00444.x

Schmid, N., Eichenberger, A. P., Choutko, A., Riniker, S., Winger, M., Mark, A. E., & van Gunsteren, W. F. (2011). Definition and testing of the GROMOS force-field versions 54A7 and 54B7. *European Biophysics Journal : EBJ*, *40*(7), 843–856. https://doi.org/10.1007/s00249-011-0700-9

Schüttelkopf, A. W., & van Aalten, D. M. F. (2004). PRODRG: a tool for high-throughput crystallography of protein-ligand complexes . *Acta Crystallographica. Section D, Biological Crystallography*, *60*(Pt 8), 1355–1363. https://doi.org/10.1107/S0907444904011679

Seo, Y., Park, K. E., Kim, Y. A., Lee, H.-J., Yoo, J.-S., Ahn, J.-W., & Lee, B.-J. (2006). Isolation of tetraprenyltoluquinols from the brown alga *Sargassum thunbergii*. *Chemical & Pharmaceutical Bulletin*, *54*(12), 1730–1733. https://doi.org/10.1248/cpb.54.1730

Sheu, J-h., Huang, S-y., Wang, G-h., & Duh, C-y. (1997). Study on cytotoxic oxygenated desmosterols isolated from the red alga *Galaxaura marginata* in a Search for Bioactive Metabolites from Marine. *Journal of Natural Products*, *60*(9), 900–903. https://doi.org/10.1021/np9701844

Trott, O. L. E. G., & Olson, A. J. (2010). AutoDock Vina: Improving the speed and accuracy of docking with a new scoring function, efficient optimization, and multithreading. *Journal of Computational Chemistry*, *31*(2), 455–461. https://doi.org/10.1002/jcc.21334

Wu, Y., Tepper, H. L., & Voth, G. A. (2006). Flexible simple point-charge water model with improved liquid-state properties flexible simple point-charge water model with improved liquid-state. *The Journal of Chemical Physics*, *124*(2), 024503–024513. https://doi.org/10.1063/1.2136877

Su, H., Yuan, Z.-H., Li, J., Guo, S.-J., Deng, L.-P., Han, L.-J., Zhu, X.-B., & Shi, D.-Y. (2009). Sesquiterpenes from the marine red alga *Laurencia saitoi*. *Helvetica Chimica Acta*, *92*(7), 1291–1297. https://doi.org/10.1002/hlca.200800437

Yun, J. W. (2010). Possible anti-obesity therapeutics from nature-A review. *Phytochemistry*, *71*(14-15), 1625–1641. https://doi.org/10.1016/j.phytochem.2010.07.011